Vol.68: e25240713, 2025
https://doi.org/10.1590/1678-4324-2025240713
ISSN 1678-4324 Online Edition

BABT
Brazilian Archives of Biology and Technology

Article - Biological and Applied Sciences

Lutein Polymeric Nanocapsules for Skin: Development and Characterization

Thais Franceni de Oliveira[1]
https://orcid.org/0009-0009-2807-6246

Romaiana Picada Pereira[2]
https://orcid.org/0000-0002-2358-2264

Brenda Alves Lopes[1]
https://orcid.org/0000-0002-4658-0333

Guilherme dos Anjos Camargo[1]
https://orcid.org/0000-0002-3440-2791

Marcela Novak Gummy[1]
https://orcid.org/0000-0001-5476-5816

Paulo Vitor Farago[1]
https://orcid.org/0000-0002-9934-4027

Elton Kazmierczak[2]
https://orcid.org/0000-0001-9654-2485

Patrícia Mathias Döll-Boscardin[1*]
https://orcid.org/0000-0001-6092-043X

Maycon Hudson Contador[2]
https://orcid.org/0009-0009-1257-7898

[1]Universidade Estadual de Ponta Grossa, Departamento de Ciências Farmacêuticas, Ponta Grossa, Paraná, Brasil;
[2]Universidade Estadual de Ponta Grossa, Departamento de Química, Ponta Grossa, Paraná, Brasil.

Editor-in-Chief: Bill Jorge Costa
Associate Editor: Bill Jorge Costa

Received: 20-Aug-2024; Accepted: 05-Feb-2025

*Correspondence: pdoll@uepg.br; Tel.: +55 42 99113-3900 (P.M.D.B.).

HIGHLIGHTS

- PCL nanocapsules containing lutein for skin use were successful obtained.
- Nanocapsules showed physical stability after 30 days when stored at room temperature and 4 °C.
- Nanoencapsulation improved the *in vitro* antioxidant action compared to free lutein.
- PCL nanocapsules containing lutein show biocompatibility with fibroblasts at lower concentrations.

Abstract: Lutein, a potent carotenoid antioxidant, shows promise for anti-aging applications. However, its vulnerability to light, heat, and oxygen, coupled with poor water solubility, hinders skin penetration and bioavailability. Nanostructured systems offer a solution to enhance stability and permeation. Our objective was to develop, characterize, and assess the cytotoxicity and antioxidant activity of polymeric nanocapsules containing lutein, using poly(ε-caprolactone) (PCL). Nanocapsules were synthesized via preformed polymer interfacial deposition method and characterized using dynamic light scattering (DLS), electrophoretic mobility, and pH. Morphology was examined using field emission scanning electron microscopy (FESEM). X-ray diffraction (XRD) indicated the crystalline structures while Fourier-transform infrared spectra (FTIR) provided information on the chemical bonds between the drug and polymer. Antioxidant activity was measured using FRAP, DPPH, and ABTS assays, while cytotoxicity was evaluated on 3T3 fibroblasts. Lutein encapsulation within PCL nanocapsules yielded spherical particles around 300 nm, with low polydispersity and zeta potential exceeding -30 mV. The pH ranged from 4.57 ± 0.03 to 5.42 ± 0.065. XRD suggested molecular dispersion of the lutein and the polymer. FTIR demonstrated the absence of chemical bonds between lutein

and PCL. Ambient and 4 °C temperatures preserved nanosystems' characteristics for 30 days. Enhanced antioxidant activity was observed in encapsulated lutein, shown by FRAP, DPPH, and ABTS assays. Results indicated that lutein nanoparticles exhibited good biocompatibility and no cytotoxicity at concentrations ranging from 61.87 µg/mL to 7.73 µg/mL. These findings emphasize the potential of lutein-loaded PCL nanocapsules for skin delivery, providing stability and antioxidant efficacy.

Keywords: Nanotechnology; nanocapsule; carotenoid; skin; anti-aging.

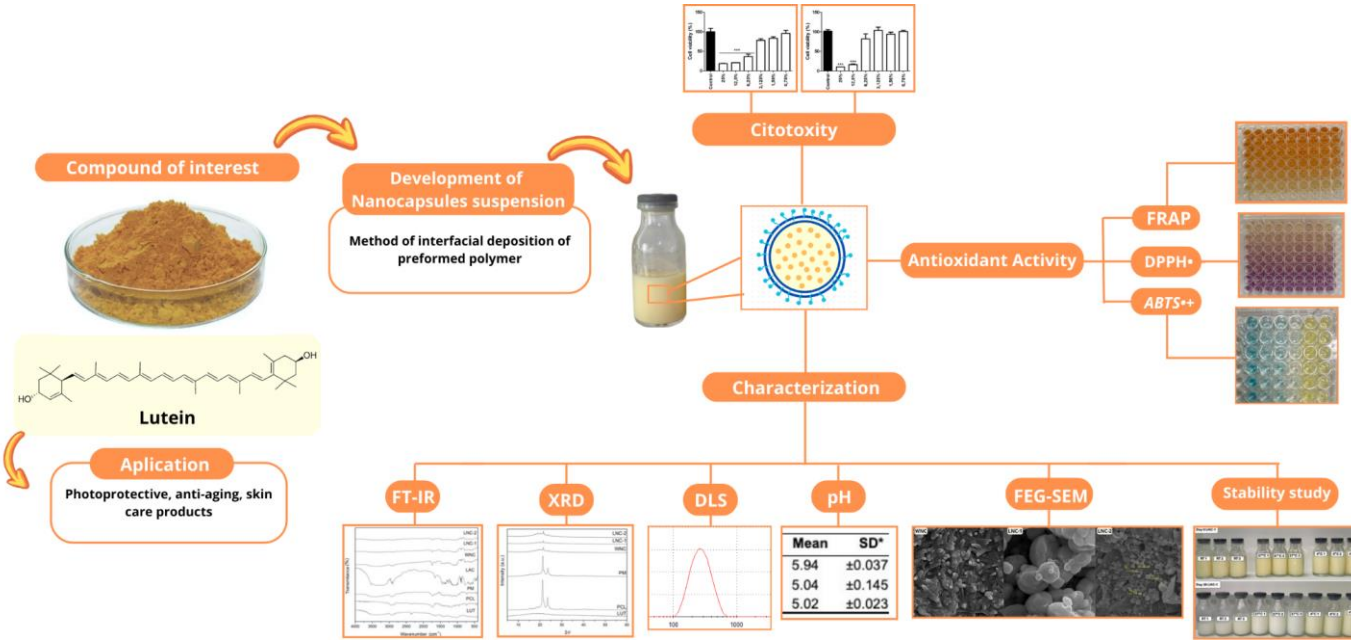

INTRODUCTION

Skin aging is a complex process influenced by genetic, epigenetic, and environmental factors, resulting in structural and physiological changes such as wrinkles, loss of elasticity, blemishes, and sagging [1,2]. Given that the skin serves as the body's largest organ and primary defense against external aggressors, understanding methods to delay or mitigate these aging signs is crucial [3-5]. Consequently, there is a growing consumer interest in anti-aging products, particularly those derived from sustainable and natural sources, with lutein emerging as a prominent contender [5-7].

Lutein, a carotenoid derived from plant secondary metabolism, has garnered recognition for its skin-related biological properties, primarily its antioxidant potential, which can help alleviate damage caused by free radicals associated with skin aging signs [5-7]. Studies suggest that lutein may shield the skin from UV damage, diminish wrinkles, enhance skin hydration and elasticity, and serve as an oral photoprotective agent [5-8]. However, lutein faces technological hurdles due to its susceptibility to heat, light, and oxygen, alongside its low aqueous solubility, resulting in reduced bioavailability and clinical effectiveness [9-11]. To address these challenges, nanoscale systems, particularly polymeric nanocapsules, have emerged as a promising solution, offering improved physicochemical stability and controlled release of lipophilic substances like lutein, thereby enhancing bioavailability and therapeutic efficacy [12-14]. These systems hold significant potential for the development of nanotechnology-based products containing natural antioxidants, offering promising avenues for maintaining youthful skin appearance over the long term [5,6,15,16].

Polymeric nanocapsules offer distinct advantages due to their encapsulated core structure. Unlike nanospheres, the oil core within nanocapsules significantly enhances drug encapsulation while minimizing the amount of polymeric matrix required. The polymeric shell serves to shield the encapsulated drug from the surrounding tissue environment, thereby preventing degradation or premature release caused by pH, temperature, enzymes, and other biological factors. Moreover, this shell can be functionalized with smart molecules capable of interacting with specific biomolecules, enabling more precise drug delivery. These benefits highlight the substantial interest and widespread application of nanocapsules in the pharmaceutical field, both as drug carriers and for cosmetic purposes [12,14,17,18].

In this vein, our study endeavors to develop, characterize, quantify, and assess the antioxidant activity and *in vitro* cytotoxicity of lutein- loaded polymeric nanocapsules, aiming to explore their suitability for topical application in addressing signs of skin aging.

MATERIAL AND METHODS

Development of PCL nanocapsule suspensions

The PCL nanocapsules (NCs) were synthesized using the interfacial deposition method of preformed polymer, following the procedure described by Fessi and coauthors [18]. Poly(ε-caprolactone) (PCL) (0.1 g) was dissolved in acetone (27 mL) with Span® 80 (0.07 g), lutein (0.08 g for LNC-1 and 0.16 g for LNC-2), and caprylic acid triglycerides (0.3 g) under mechanical stirring at 40°C until fully dissolved. Next, the organic phase was gradually added dropwise to the aqueous phase (53 mL) containing Tween® 80 (0.077 g). The resulting suspension was stirred magnetically at 40°C for 40 minutes. The organic solvent was subsequently removed using a rotary evaporator (Quimis, São Paulo, Brazil) resulting in a final volume of 10 mL (1.5 mg/mL), as depicted in Figure 1. Additionally, a suspension of nanocapsules without the drug (WNC) as negative control was prepared, and all formulations were replicated three times for comparative analysis.

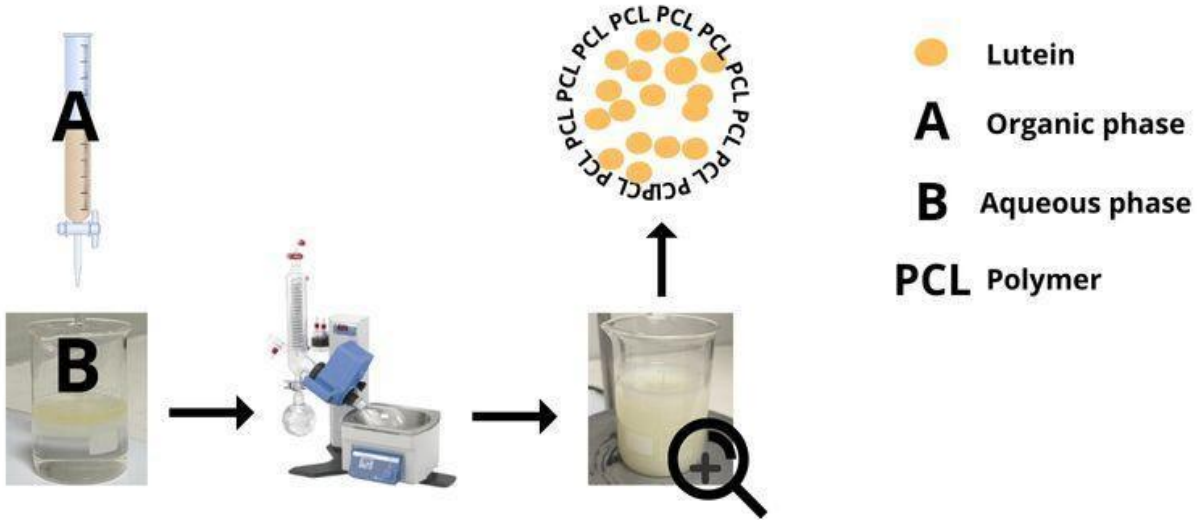

Figure 1. Diagram illustrating the process for producing polymeric nanocapsules containing lutein, prepared via interfacial deposition of the preformed polymer.

Physicochemical characterization

Determination of Mean Diameter, Polydispersity Index (PDI), Zeta Potential and pH

The mean particle size, polydispersity index (PDI), and zeta potential were determined (n = 3) after diluting a sample of the nanocapsule suspension in ultrapure water at a 1:500 ratio. All measurements were conducted using the Zetasizer® Nano ZS90 (Malvern Instruments, Malvern, United Kingdom).

pH values were measured using a digital potentiometer (Digimed®, Brazil), which had been previously calibrated with pH 4.0 and 7.0 buffer solutions. The pH was directly measured in each colloidal suspension after its preparation.

Statistical differences between the mean values were assessed through a one-way analysis of variance (ANOVA) followed by Tukey's post-hoc test with the software GraphPad Prism® version 6.01 program (San Diego, CA, USA).

Morphological and structural characterization

Field Emission Scanning Electron Microscopy (FESEM) Analysis

The PCL NCs formulations were previously prepared using lactose monohydrate as a cryoprotectant. In brief, 1 g of lactose was dissolved in 10 mL of the NCs formulations under magnetic stirring. The resulting suspension was frozen at -80 °C for 24 hours in a ULT upright freezer (Thermo Scientific, model ULT-2186-3-D37, Waltham, MA, USA). Subsequently, the frozen samples were freeze-dried in a lyophilizer (LIOTOP, L202, São Paulo, Brazil) for 48 hours to ensure complete water removal. The freeze-dried samples were

sputter-coated with gold using an IC-50 ion coater metallizer (SHIMADZU,Kyoto, Japan). Morphological evaluation of the NCs was carried out and images were prepared using a FESEM (TESCAN, model Mira 3, Brno, Czech Republic) at an acceleration voltage of 8 to 10 kV.

X-ray Diffraction Analysis

Pure lutein (LUT), PCL, physical mixture (PM) and NCs were analyzed using a Shimadzu XRD-6000 X-ray diffractometer. To carry out this analysis, the nanosuspension samples were dropped on a slide and dried at room temperature to obtain a thick layer of sample. The experiments were performed at scanning rate of 2º/min and a range from 4º to 80º using copper Kα radiation (λ = 1.5418 Å), current of 40mA and voltage of 40kV to observe possible peaks indicative of crystallinity.

FTIR Spectroscopic Analysis

The lyophilized LNC-1 and LNC-2 formulations were examined using Fourier-transform infrared spectroscopy (FTIR) with potassium bromide (KBr) pellets. Each pellet was composed of 4 mg of the sample and 196 mg of spectroscopic grade KBr (2%, m/m). The analysis was conducted using IR Prestige-21 equipment (SHIMADZU, Kyoto, Japan) over a range of 4000-400 cm^{-1}, with a resolution of 4 cm^{-1} and a scanning rate of 32 scans per minute. The resulting spectra were then compared with those of the pure drug (lutein), the polymer, and the negative control formulation (WNC).

Physicochemical stability

LNC-1, LNC-2 and WNC suspensions underwent evaluation under various storage conditions, including protection from light, at room temperature (25°C), in an oven at 37°C, and in a refrigerator at 4°C for 30 days. Measurements were conducted at 0, 10, 15, and 30 days within a temperature range of 4°C to 37°C to evaluate pH, particle size, polydispersity index (PDI), and zeta potential. All analyses were performed in triplicate. Stability data were analyzed using GraphPad Prism® version 6.01 for Windows. Results are presented as mean ± standard deviation. Statistical comparisons were conducted using ANOVA with Bonferroni post-test for multiple comparisons, with a significance level set at 5% (α = 0.05).

Radical Scavenging Activity

Ferric-Reducing Antioxidant Power (FRAP)

The Ferric-reducing Antioxidant Power (FRAP) assay, as described by Berker and coauthors [19], comprised several procedural steps. Firstly, ammonium ferric sulfate dodecahydrate ($NH_4Fe(SO_4)_2 \cdot 12\ H_2O$) (160.0 mg) was dissolved in hydrochloric acid (1 M HCl) (2 mL). Then, ultrapure water (50 mL) and 1,10-phenanthroline (180.2 mg) were added. The volume was adjusted to 100 mL with ultrapure water in a flask, resulting in a final concentration solution of $1.10x10^{-2}$ mol L^{-1}. Next, the two solutions were combined and diluted with 100 mL of ultrapure water. In test tubes, 0,25 mL of samples diluted in acetone to a concentration of 1:4 and 2 mL of the Fe^{3+}-1,10-phenanthroline complex solution were added. The tubes were subsequently incubated in darkness for 30 minutes until the reaction reached completion. Absorbance readings were measured at 510 nm using a UV-Vis spectrophotometer against reagent blank. For negative control, the procedure was repeated without adding the samples. Ascorbic acid was employed as a control to establish the calibration curve, with concentrations ranging from 10 to 0 ppm (8, 6, 4, 3, 2, and 0 ppm included). The results were expressed as micrograms of ascorbic acid equivalent per milliliter of sample ($AA\mu g/mL^{-1}$).

DPPH free radical scavenging activity

Based on Brand-Williams and coauthors [20], the control curve construction consisted of a standard sample of ascorbic acid following concentrations of 10, 8, 6, 4, 3, 2, and 0 ppm. Solutions of the samples were prepared in acetone at a ratio of 1:4. In test tubes, 2 mL of each sample and 2 mL of DPPH• solution (120 µmol/L) in acetone were added. A negative control was also performed by adding 1 mL of DPPH in triplicate and 1 mL of acetone. After curve construction and addition of samples and DPPH, the tubes were incubated in darkness for 30 minutes to allow the reaction to complete. The samples were measured at 517 nm using a UV-Vis spectrophotometer. Results were reported as micrograms of ascorbic acid equivalent per milliliter of sample ($AA\mu g/mL^{-1}$).

ABTS free radical scavenging activity

ABTS (2,2-azino-bis(3-ethylbenzothiazoline-6-sulfonic acid)) was used to evaluate radical cation scavenging activity. According to the procedures outlined by Re and coauthors [21] and Shu and coauthors [22], a stock solution of ABTS was prepared at a concentration of 7 mmol L^{-1} by combining 88 µL of potassium persulfate (2.45 mmol L^{-1}) ($K_2 S_2 O_8$). The prepared solution was kept in darkness at -20°C (freezer) for 16 hours to allow the ABTS•+ radical formation. Afterward, the solution was diluted in ethanol to attain an absorbance of 0.70 at 734 nm, as determined using a spectrophotometer, before application. To create the standard curve, ascorbic acid was added to a 96-well microplate at concentrations of 10, 8, 6, 4 , 3, 1 and 0 ppm. Then, the analysis samples underwent dilution in a 1:4 ratio. Next, the diluted samples (1000 µL) $ABTS^{\bullet+}$ (3000 µL) were combined in test tubes, and this mixture (300 µL) transferred to microplates. The microplates were then incubated for 30 minutes away from light before absorbance readings at λ 734 nm were taken using a spectrophotometer. A solution of 300 µL of the $ABTS^{\bullet+}$ solution acted as the negative control. The results were reported as the equivalent antioxidant activity of ascorbic acid per milliliter of sample (AAµg/mL-1). For the antioxidant activity assessments, after performing ANOVA, the group means were compared using the student-Newman-Keuls test through the GraphPad Prism® version 6 software (San Diego, CA, USA). A significance level of $p < 0.05$ was considered. Pearson correlation was used to calculate the data correlations.

Cell viability test

The cells used were 3T3 mouse fibroblasts, which were cultured in Dulbecco's Modified Eagle Medium (DMEM) containing fetal bovine serum (FBS) (10%). They were planted in 96-well plates at a density of $2x10^5$ cells/well and maintained in an incubator at 37°C with 5% CO_2 for 24 hours. After this period, supernatant was discarded, the NCL-1 sample were added to the plate at concentrations of 247.50 µg/mL, 123.75 µg/mL, 61.87 µg/mL, 30.93 µg/mL, 15.46 µg/mL, and 7.73 µg/mL, corresponding to 25%, 12.50%, 6.25%, 3.12%, 1.56%, and 0.78%, respectively. For NCL-2, the same concentrations were used. The concentrations were obtained by diluting the formulations in DMEM (FBS 10%). Following a 24-hour incubation at 37°C in a humidified atmosphere with 5% CO2, the cells treated with the samples had their supernatant removed, and an MTT solution was introduced to the cells. Afterwards, the formazan crystals were dissolved in dimethyl sulfoxide (DMSO), and their absorbance was measured at 570 nm using a plate reader. DMEM was employed as negative control, and cell viability was assessed by comparing the cells treated with the samples to those untreated cells (negative control).

Statistical analysis

The analyses were carried out in triplicate and results are presented as mean ± standard deviation ($n = 3$). Statistical analysis was conducted using two-way ANOVA, followed by Tukey's post-hoc multiple comparisons test, performed with GraphPad Prism version 5.04 software (San Diego, California, USA). A significance level of $p < 0.05$, $p < 0.01$ and $p < 0.001$ was applied for statistical evaluation.

RESULTS

Development of polymeric nanocapsules

LUT-loaded PCL nanocapsules (LNC-1, LNC-2) and negative control nanocapsules (WNC) were successfully prepared using the interfacial deposition method. Both LNC-1 and LNC-2 suspensions exhibited a milky, homogeneous appearance with opalescent yellowish-white color and a lutein odor, while WNC displayed a milky, homogeneous appearance with opalescent white color. Additionally, all formulations exhibited bluish reflections, indicative of the Tyndall effect, resulting from light reflection on nanoscale particles [12,18]. Importantly, none of the analyzed formulations exhibited phase separation or crystal formation.

Characterization of NCs

Determination of Mean Diameter, Polydispersity Index (PDI), Zeta Potential and pH

Table 1 displays the mean particle size, polydispersity index (PDI), zeta potential (ZP), and pH results for LNC-1, LNC-2, and WNC, presented as the mean and standard deviation (SD). The formulations showed nanometer-sized particles, which are typical for this type of system, and were characterized by PDI values

below 0.5, indicating monodispersity. The zeta potential values for both NC suspensions were negative. Statistical analysis indicated significant differences between these nanoformulations in terms of zeta potential and pH.

Table 1. Results obtained for the physical-chemical characterization of NCs suspensions.

Formulation	Mean diameter (nm)		Polydispersity Index (PDI)		Zeta Potential (mV)		pH	
	Mean	SD	Mean	SD	Mean	SD	Mean	SD
WNC	277.40	± 7.00	0.214	± 0.061	-37.4	±3.88	5.94*	±0.037
LNC-1	290.30	± 16.36	0.220	± 0.062	-37.3	±1.57	5.04	±0.145
LNC-2	296.33	± 26.29	0.229	± 0.038	-19.16*	±8.14	5.02	±0.023

* $p<0.05$.

Field Emission Scanning Electron Microscopy (FESEM) Analysis

Figure 2 displays photomicrographs obtained through FESEM of the nanoformulations, showing particles with a well-defined spherical shape and a smooth, uniform surface. The particle diameters are consistent with those measured by DLS, being less than 300 nm. Additionally, lutein was not detected on the particle surfaces, indicating effective encapsulation within the nanocapsules.

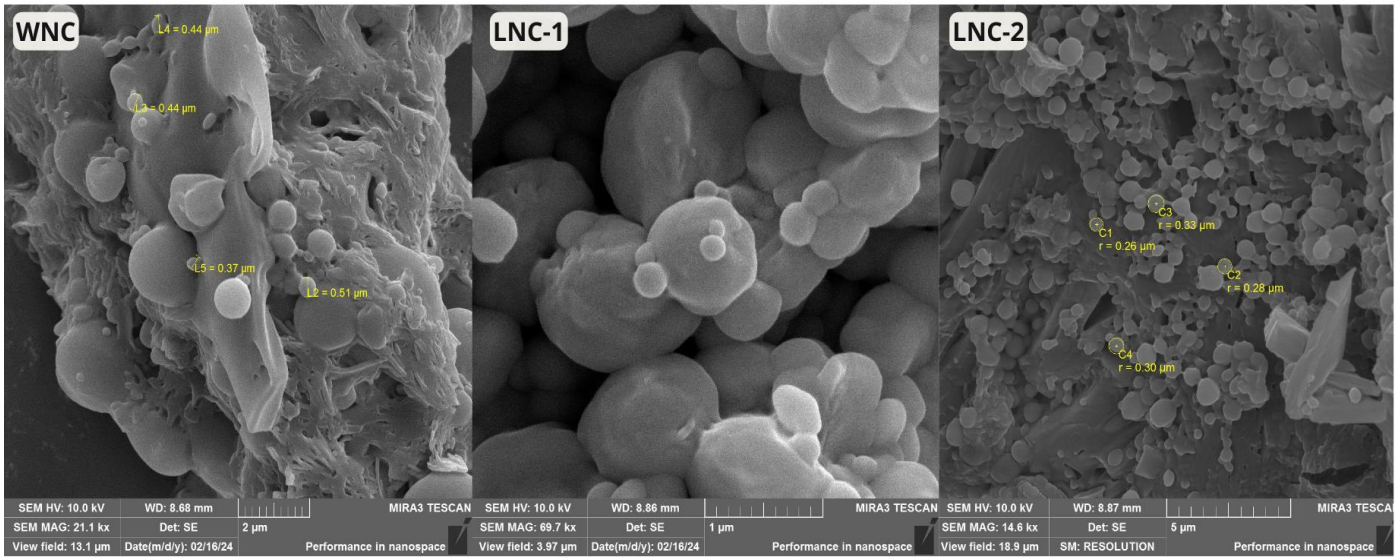

Figure 2. Photomicrographs of freeze-dried Lutein nanocapsules WNC at 21.100 x magnification, LNC-1 69.700 x magnification, and LNC-2 14.600 x magnification.

X-ray Diffraction Analysis

The XRD characterization identified whether the materials were crystalline or amorphous. Figure 3 presents the XRD data for pure lutein, PCL, lactose, physical mixture (PM), WNC, LNC-1, and LNC-2. Pure lutein exhibited an amorphous pattern, indicated by the absence of peaks and the presence of a broad band. In contrast, the PCL demonstrated its semi-crystalline nature with characteristic peaks at 2θ of 21.45 and 23.73° [23,24]. The PM displayed crystallinity peaks that corresponded with those observed for the polymer and drug.

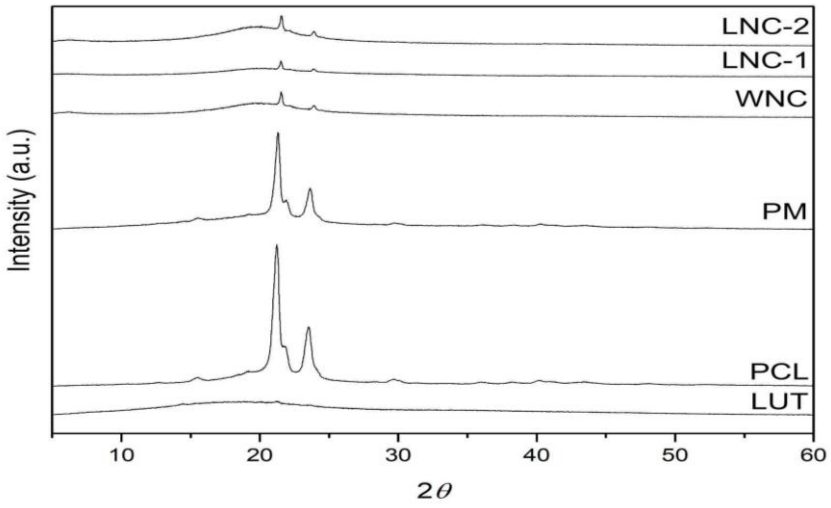

Figure 3. X-ray diffractograms of pure lutein, PCL, lactose, physical mixtures of lutein/PCL, and nanoformulations LNC-1, LNC-2, and WNC.

For the nanoformulations LNC-1 and LNC-2, no crystallinity of the drug was detected, suggesting that lutein remained in an amorphous state during the interfacial deposition process with the preformed polymer method. All nanoformulations showed PCL semi-crystallinity peaks at 2θ of 21.45 and 23.73° [23,24].

FTIR Spectroscopic Analysis

Figure 4 displays the FTIR spectra for lutein, PCL, physical mixture (PM), lactose, WNC, LNC-1 and LNC-2. Lutein's characteristic infrared absorptions were observed as an O–H stretching vibration at 3000 cm-1, C–H stretching peaks at 2918 cm-1 and 2848 cm-1 and C–C stretching peaks at 1715 cm-1 [25,26]. The FTIR spectrum of PCL exhibited characteristic bands including sp3 hybridized carbon stretch vibrations at 2948 cm-1, 2899 and 2865 cm-1, an ester C=O stretch vibration at 1729 cm-1, sp3 hybridized carbon angular vibrations at 1740 cm-1, C–O symmetric stretch vibrations at 1297 and 1241 cm-1, an asymmetric C–O stretch at 1175 cm-1 and sp3 hybridized carbon angular vibrations at 731 cm-1 [24]. The absorption bands attributed to the PM corresponded to the superposition of the FTIR spectra of the pure drug and the polymer without any change.

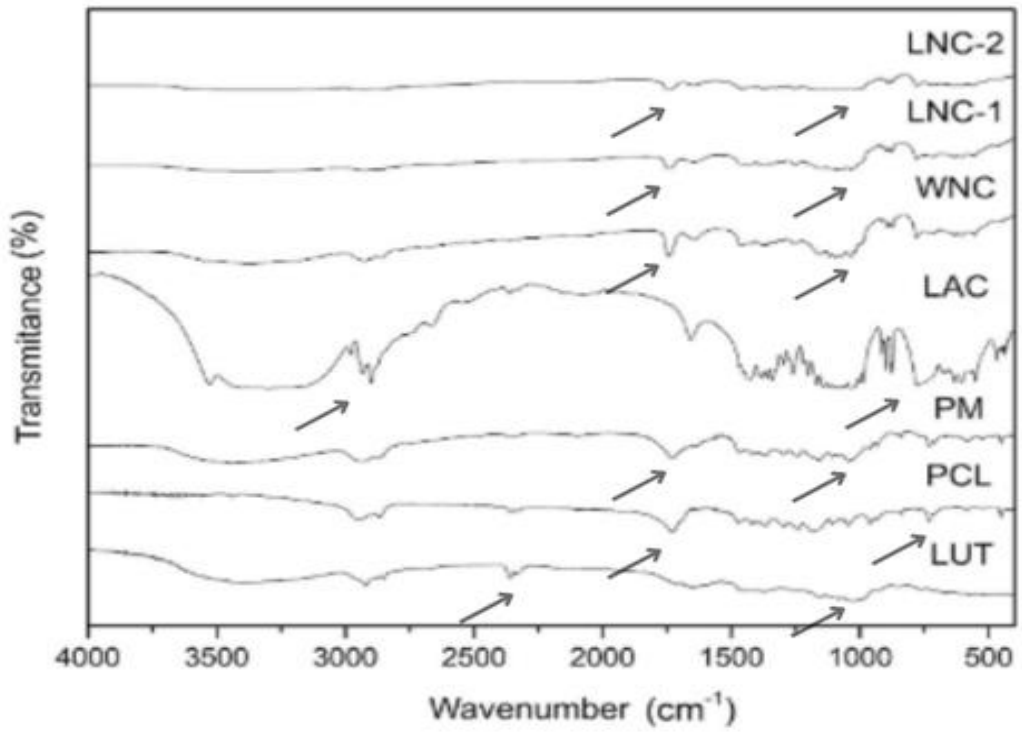

Figure 4. FTIR spectra of pure lutein, PCL, lactose, physical mixing lutein/pcl, nanoformulations LNC 1 and 2 and WNC.

Lactose used for lyophilization exhibited an OH stretch vibration band at 3530 cm^{-1} due to intermolecular hydrogen bonding, along with a broad OH signal at 3300 cm^{-1}. The sp3 hybridized carbon stretch vibrations were observed at 2980, 2934, 2898 and 2879 cm^{-1}, while the O–C stretch vibration/asymmetric C–O–C stretch of ether was not noted at 1035cm^{-1}, and the OH angular vibration was identified at 775cm^{-1} [24].

Comparing the spectra of unloaded NCs with those of NCs loaded with lutein, signals associated with lactose used for lyophilization, including the OH angular vibration at 775 cm^{-1}, were confirmed. Additionally, bands corresponding to PCL were observed, primarily due to the C=O stretching vibration of the polymer at 1743 cm^{-1}. The minor shift in the C=O stretching vibration of the PCL from the pure polymer's peak at 1729 cm^{-1} is likely attributed to the NCs preparation method used for the analysis. No FTIR signals for lutein were detected in the LNC-1 and LNC-2 spectra, which may indicate that the drug is encapsulated.

Physicochemical stability

During the stability study period, all nanosuspensions maintained the same initial milky appearance characteristic of nanocapsules in colloidal suspension, exhibiting good physicochemical stability, and the absence of creaming, sedimentation, or flocculation processes, as observed in Figure 5 [12,17,27].

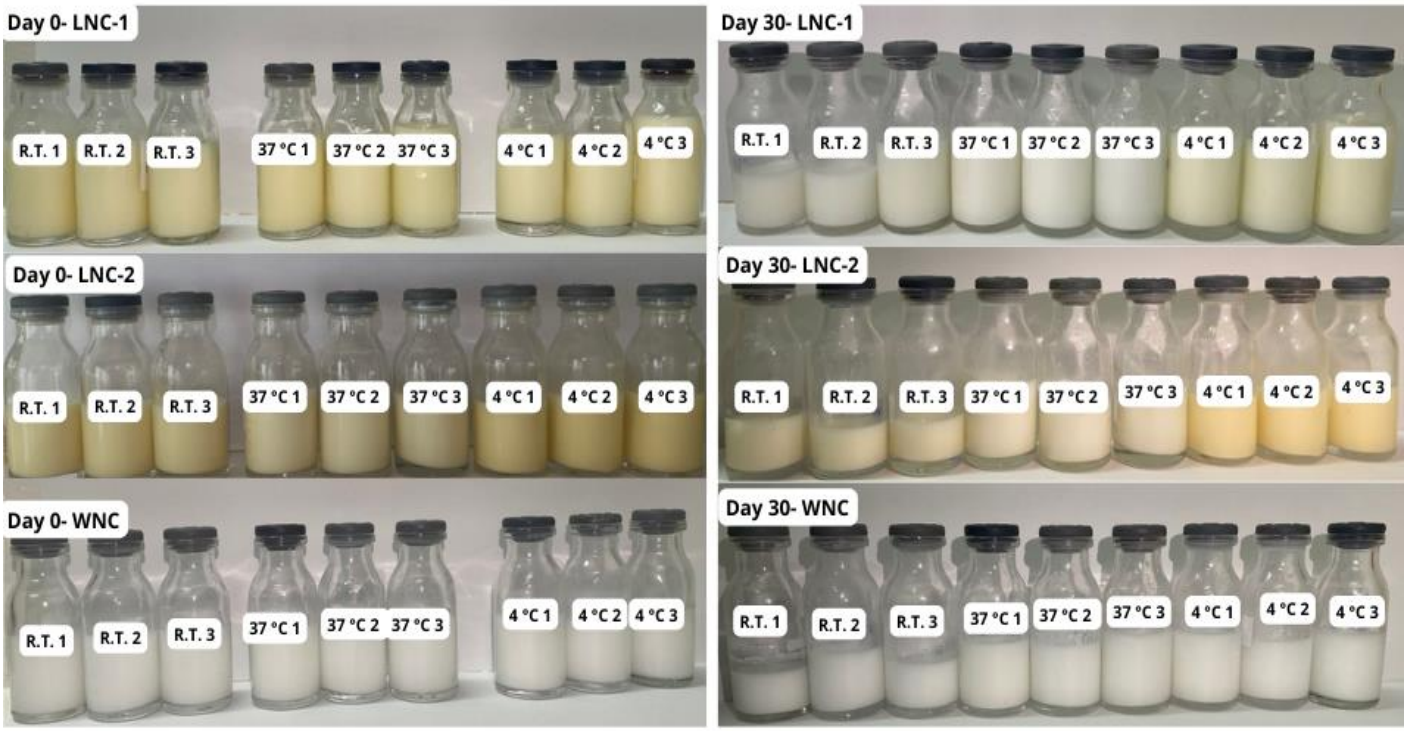

Figure 5. Macroscopic aspects of the NCs (LNC-1, LNC-2, and WNC) stored at room temperature (R.T.), 37 °C (oven), and 4 °C (fridge) for the stability study (30 days).

In summary, the values of size, PDI, zeta potential, and pH did not show significant differences that would compromise the stability of the nanoformulations for samples with lutein (LNC-1 and LNC-2) and without lutein (WNC) as observed in Figures 6 to Figure 9 at room temperatures and at 4 °C.

Figure 6 demonstrated that samples LNC-1, LNC-2, and WNC showed no significant changes in their sizes over time, suggesting absence of coalescence and degradation of the samples, as confirmed by macroscopic analysis (Figure 5). From the 15th day onwards, samples stored at 37°C exhibited larger particle sizes compared to the same samples stored at room temperature and in the refrigerator.

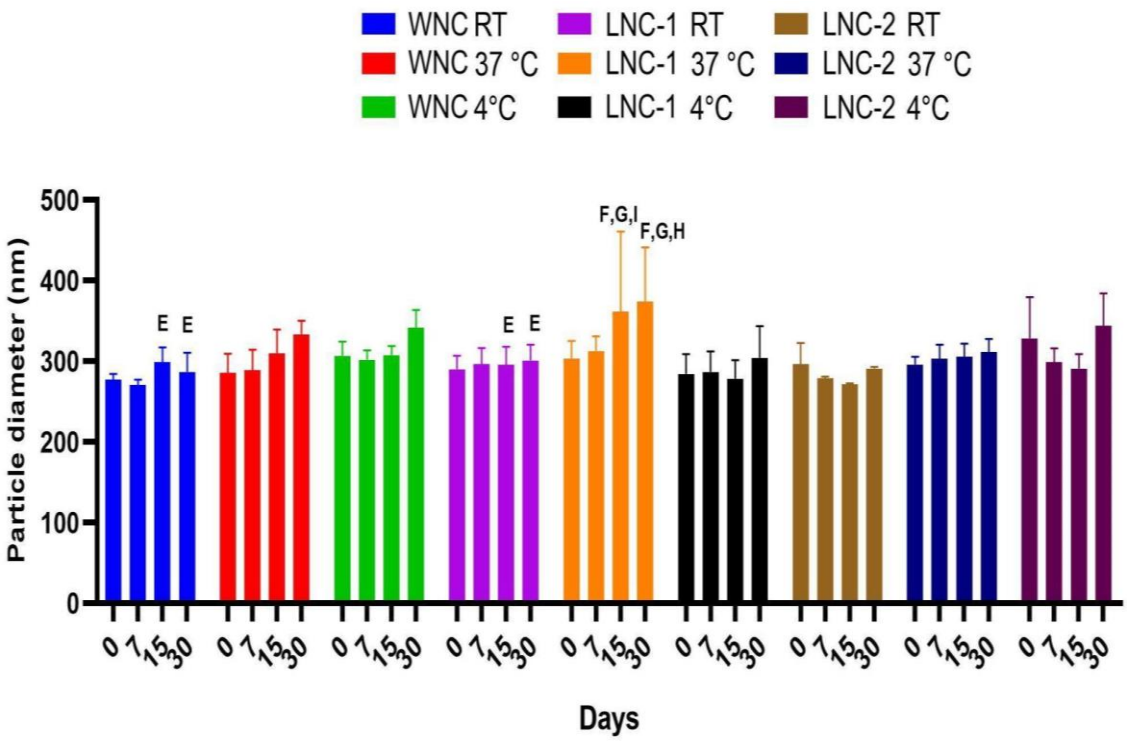

Figure 6. Stability studies of LNC-1, LNC-2, and WNC were conducted, focusing on particle diameter in nm. Room temperature (R.T.). Statistical significance was determined with *p < 0.05. E) comparison with LNC-1 stored at 37°C; F) comparison with LNC-1 stored at 4°C. G) comparison with LNC-2 stored at R.T.; H) comparison with LNC-2 stored at 37°C.

The polydispersity index (PDI), as shown in Figure 7, increased in all samples over the study period, especially for samples stored at 37°C. Zeta potential revealed electrostatic stability, with values close to -30 mV even after 30 days of storage (Figure 8). Significant differences were observed in the zeta potential between samples without lutein and those with lutein at different temperatures, indicating that the presence of lutein reduced the zeta potential, making it more positive.

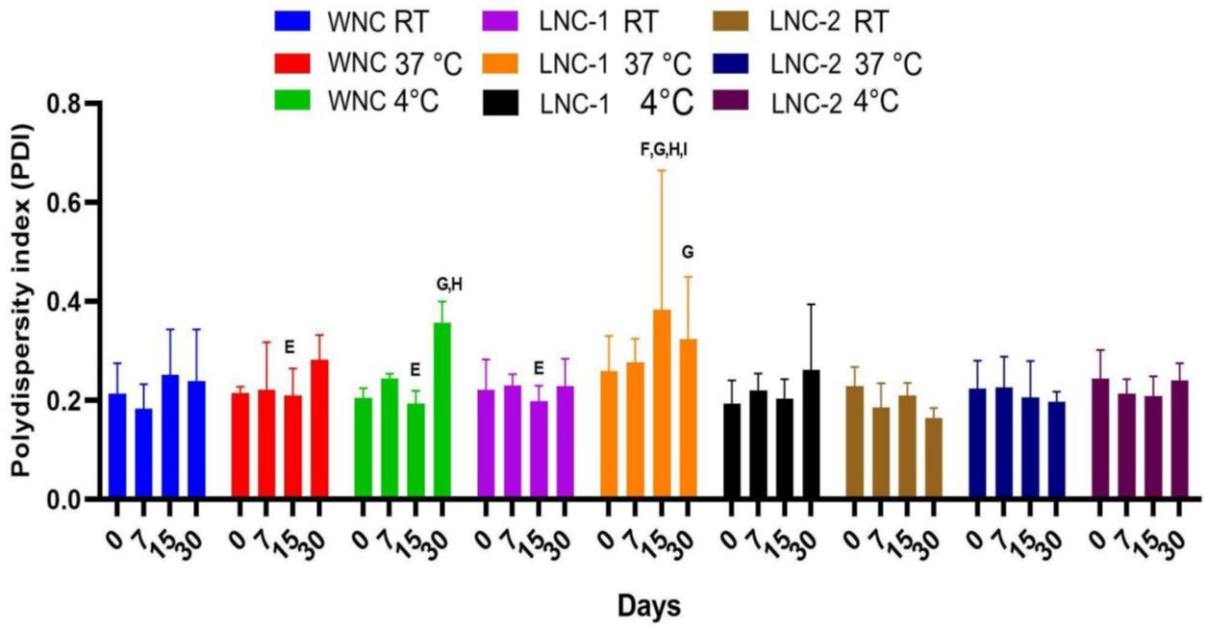

Figure 7. Stability studies of LNC-1, LNC-2, and WNC based on the polydispersity index (PDI). Room temperature: (R.T.). Statistical significance was determined with *p < 0.05. E) comparison with LNC-1 stored at 37°C; F) comparison with LNC-1 stored at 4°C. G) comparison with LNC-2 stored at room temperature; H) comparison with LNC-2 stored at 37°C; I) comparison with LNC-2 stored at 4°C.

The LNC-1 at different temperatures and compared to LNC-2 at different temperatures showed significant differences in zeta potential. Despite the differences observed in Figure 8, all samples exhibited zeta potential values close to -30 mV under all conditions over the 30 days, including samples stored at 37°C.

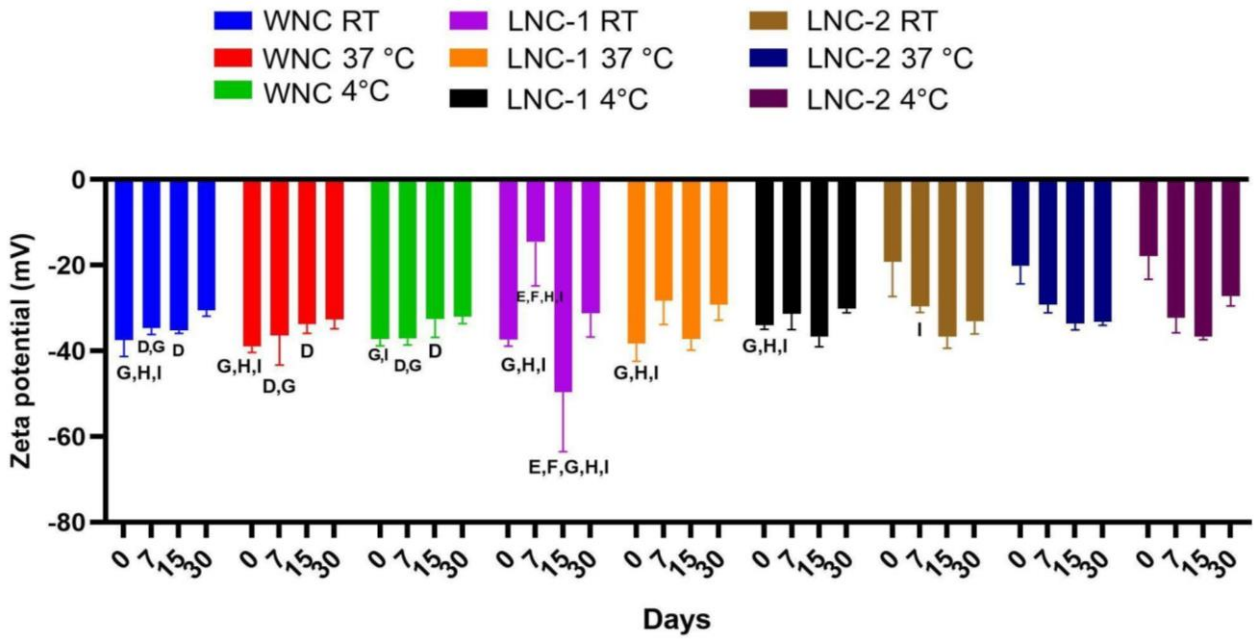

Figure 8. Stability studies of the LNC-1, LNC-2 and WNC depending on the zeta potential (mV). Room temperature: (R.T.). Statistical significance was determined with *p < 0.05; D) comparison with LNC-1 stored at room temperature; E) comparison with LNC-1 stored at 37°C; F) comparison with LNC-1 stored at 4°C. G) comparison with LNC-2 stored at room temperature; H) comparison with LNC-2 stored at 37°C; I) comparison with LNC-2 stored at 4°C.

The WNC samples stored at room temperature, 37°C, and 4°C maintained a pH close to 6 throughout the 30-day study period, with WNC at 4°C showing less variation in pH during the analyzed period as observed in Figure 9. LNC-1 samples stored at room temperature and 4°C maintained relatively stable pH over time, with pH close to 5, while LNC-1 stored at 37°C showed a more pronounced decrease in pH over the days, with a pH value of 3.46 ± 0.081 on day 30. The same behavior is observed for LNC-2 samples, where samples stored at room temperature and 4°C maintained pH close to 5, while at 37°C, the pH value was 3.47 ± 0.102 on day 30.

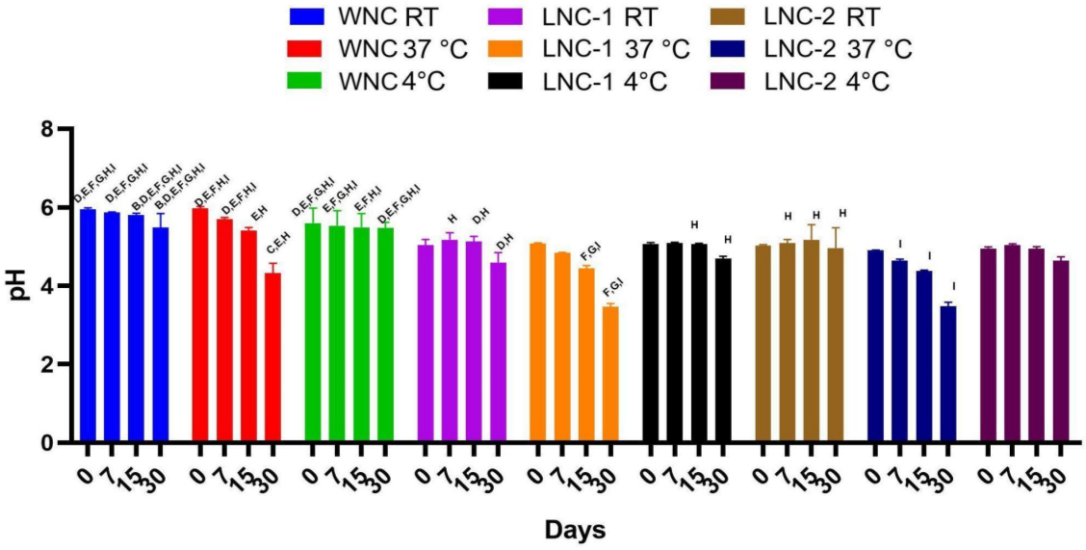

Figure 9. Stability study of the LNC-1, LNC-2 and WNC depending on the pH. Room temperature: R.T.*p < 0.05;B) comparison with WNC stored at 37°C; C) comparison with WNC stored at 4°C; D) comparison with LNC-1 stored at room temperature; E) comparison with LNC-1 stored at 37°C; F) comparison with LNC-1 stored at 4°C. G) comparison with LNC-2 stored at room temperature; H) comparison with LNC-2 stored at 37°C; I) comparison with LNC-2 stored at 4°C.

At the end of the analysis period, LNC-1 and LNC-2 stored at room temperature and 37°C showed a change in color from yellow to white (Figure 6), possibly due to lutein oxidation favored at higher storage temperatures, causing physical changes in the nanocapsules.

Radical Scavenging Activity

The techniques employed to assess antioxidant activities were DPPH• and ABTS•+ radical scavenging methods, along with ferric reducing antioxidant power (FRAP). Antioxidant activities of free lutein, WNC and loaded-lutein LNCs (LNC-1 and LNC-2) were determined and shown in Table 2. In all methods studied, it is observed that LNCs are able to load the lutein without losing its antioxidant capacity. In FRAP and $ABTS^{\bullet+}$ assays, the antioxidant activity increased from WNC to LNC-2. For other side, in $DPPH^{\bullet}$ assay, the value was improved just from WNC to LNC-2, it indicated the contribution of concentration of lutein load in LNC-2. In $ABTS^{\bullet+}$ assay, however, there is a decrease between free-lutein and WNC and LNCs.

Table 2. Antioxidant activities of free-lutein, WNC, LNC-1 and LNC-2

Sample	FRAP (μg AA mL^{-1} sample)*	$DPPH^{\bullet}$ (μg AA mL^{-1} sample)*	$ABTS^{\bullet+}$ (μg AA mL^{-1} sample)*
Free-lutein	539.38 ± 10a	1186.99 ± 24.32c	418.12 ± 21.46a
WNC	48,43 ± 7.96b	2825.25 ± 19.28a	37.01 ± 3.04c
LNC-1	267.84 ± 13.86c	2780.73 ± 7.51a	65.24 ± 0.34c
LNC-2	556.30 ± 3.84a	2966.43 ± 23.88b	148.21 ± 5.7b

*Data are shown as mean ± SD (n = 3) from triplicate experiments. *Different letters (a–e) in the same column denote statistically significant differences (Newman–Keuls test, $p < 0.05$). It applied Tukey's test level 5% probability.

Cell viability test

Cytotoxicity evaluation of the polymeric nanocapsules with lutein (LNC-1 and LNC-2) in mouse 3T3 fibroblasts cells with a 24-hour exposure period is demonstrated in Figure 10.

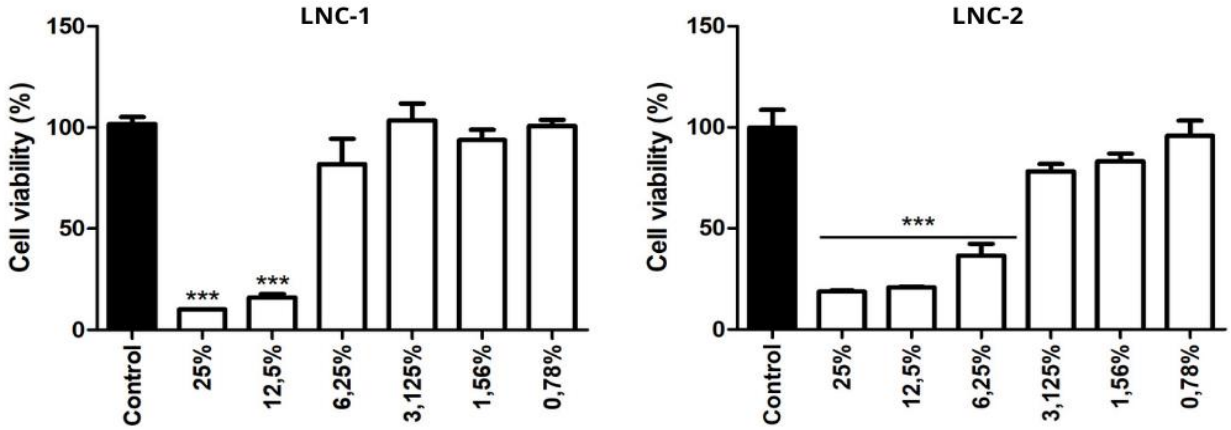

Figure 10. Effect of lutein nanocapsules (LNC-1 and LNC-2) on the viability of 3T3 fibroblasts after 24 hours, assessed by the MTT method. DMEM was employed as negative control. The data are presented as mean ± SEM (n = 8). ANOVA, accompanied by Tukey's post-hoc test, was used for the analysis. *** $p < 0.001$ in comparison with the control group.

For LNC-1 in the concentrations from 25.0 % to 12.5% there was observed decline in cell viability with $p<0,001$. Meanwhile, concentrations between 6.25% and 0.78%, no significant variation in cell viability was observed across the different concentrations of LNC-1 tested compared to the control, indicating that at concentrations lower than 123.75 μg/mL, the nanoformulation was not cytotoxic. In contrast, LNC-2 showed toxicity at concentrations from 25% to 6.25% ($p<0.001$), which is justified by it having double the lutein concentration in its composition compared to LNC-1. Thus, the PCL polymeric nanocapsules containing lutein did not exhibit any significant cytotoxicity at concentrations lower than 30.93 μg/mL, indicating that the nanoformulations are safe.

DISCUSSION

According to Schaffazick and coauthors [12], polymeric nanoparticles typically exhibit diameters ranging from 100-300 nm. These dimensions are influenced by various factors, including formulation composition, preparation method, core oil properties, polymer characteristics, surfactant types and concentrations, and the presence or absence of active ingredients.

The nanocapsules developed presented mean size consistent with the expected size range (200−500 nm) for polymer formulations prepared by the method of deposition of preformed polymer [14,17,24,28].

The Polydispersity Index (PDI) provides insights into the uniformity of particle diameters within a suspension. Samples with a PDI below 0.5 are considered monodisperse, while those with values exceeding 0.5 are classified as polydisperse [29,30]. In our study, the suspensions exhibited PDIs ranging from 0.229 ± 0.038 (LNC-2) to 0.214 ± 0.061 (WNC), indicating monodispersity. This minimal variance in particle sizes further supports their homogeneity.

Zeta potential measurements reflect the electrostatic stability of particles, with values exceeding ±30 mV indicative of adequate surface charge. This stability arises from strong repulsive forces that deter particle aggregation upon collision.

The samples presented pH between 5.02 ± 0.023 to 5.94 ± 0.037. These values are similar to the skin's pH, making them suitable for topical formulations due to their demonstrated biocompatibility, making it an interesting aspect since the objective of the work aims at the topical application of lutein in a nanostructure-controlled release [31,32].

Thus, particle size and surface properties are critical factors in the bioactivity of nanocapsules, affecting *in vitro* drug release. Reduced particle sizes create a more extensive surface area, facilitating the quick release from these nanosystems and thereby enhancing their pharmacokinetics and therapeutic efficacy. This makes them a viable option for delivering lutein across the epidermis to combat signs of skin aging, as their size is smaller than 500 nm, enabling penetration into the skin [29,33]. The characteristics observed in the FESEM images match those reported in previous studies for polymeric PCL nanoparticles. Camargo and coauthors [24] described similar features in the development of tacrolimus nanoparticles, Ferreira and coauthors [34] in diphenyl diselenide nanoparticles, and Yingngam and coauthors [35] in the synthesis of menthol nanocapsules. They all noted the presence of a reservoir structure characteristic of nanocapsules, with a lighter region in the upper portion corresponding to the polymeric wall coating and a darker central region representing the core. This distinctive feature is attributed to the presence of PCL, which forms a polymeric coating around the oily mixture of Span® 80, caprylic acid, and lutein [36].

In the XRD, the similar profiles obtained for the formulations suggest molecular dispersion between the lutein and the polymer, resulting in nanoparticles with a semi-crystalline nature, with crystallinity peaks coincident with those observed for the polymer (PCL), indicating that lutein is encapsulated within a PCL shell [24,29,37].

The FTIR analysis revealed the disappearance of the characteristic bands of lutein, suggesting its encapsulation within the polymeric matrix. No significant changes were observed in the main bands compared to the spectra of the isolated substances, indicating the absence of physicochemical interactions capable of altering the structure of the drug or the polymer. These findings, supported by the XRD results, reinforce the hypothesis that lutein is completely encapsulated, with the polymer solely functioning as a drug carrier [24,37].

The stability study conducted at different temperatures verified the behavior of these nanocapsules. Although these nanostructures are temperature-sensitive due to the effect on the droplet movement, the tendency for droplets aggregation is lower compared to formulations on larger scales, such as the macroemulsions and/or the vehiculation of lutein without appropriate formulation [11,12,14,36,38]. Figure 6 shows that there was no significant difference in the particle size of the analyzed samples (WNC, LNC-1, and LNC-2) when stored at room temperature and in the refrigerator, indicating that the nanocapsules did not undergo changes over time. This suggests that there was no coalescence or degeneration of the samples, regardless of the presence of lutein in the composition of the nanocapsules under the analyzed conditions [30].

Figure 8 shows us that this difference in PDI among samples did not harm the system, as the values remained acceptable, i.e., less than 0.3, which is satisfactory for topical use. It demonstrates that the samples remained in a unimodal distribution of their average diameters, indicating that over time, the samples continued to disperse without aggregation or flocculation occurring [30,39]. Time and storage conditions influence the zeta potential, especially at 37 °C, where variations are more pronounced, suggesting potential changes in the electrostatic stability of the nanocapsules under these conditions, likely due to polymer

degradation and alterations in the exposure of positive charges to high temperatures [40]. Despite observed differences, zeta potential values close to -30 mV (even for samples stored at 37 °C) indicate that the nanocapsules are electrostatically stable structures.

The significant differences observed indicate that pH was influenced by both storage conditions and the presence of lutein (Figure 9). Elevated temperatures and higher lutein concentration led to a decrease in the system's pH. Overall, samples stored at 37 °C showed a more pronounced decrease in pH over time, indicating potential changes in the stability of the nanocapsules under these conditions. It can be explained by the hydrolysis of medium-chain triglycerides composing the core or the surfactant released from the interface when polymer aggregates or lutein degradation products are influenced by increased temperature [10,11,40]. Samples stored at room temperature and 4 °C maintained a more stable pH throughout the study period.

At the end of the analysis period, LNC-1 and LNC-2 stored at room temperature and 37 °C showed a change in color from yellow to white (Figure 5), possibly due to lutein oxidation, which is favored at elevated storage temperatures, causing physical changes in the nanocapsules.

It has been reported in the literature that due to conjugated double bonds and hydroxyl groups in lutein, it is susceptible to oxidation when exposed to air and light, generating colorless products [10,11,26]. In contrast, LNC-1 and LNC-2 stored at 4 °C showed no macroscopic changes.

The findings are in agreement with Álvarez-Henao and coauthors [41], who observed that lutein degrades rapidly, showing a 70% reduction in three days. Encapsulated lutein, however, demonstrated only 39% degradation after 21 days at 25°C. After 21 days at 50°C, the nanoparticle containing lutein preserved around 20% of the encapsulated lutein, while the physical mixture retained only 1% of the lutein. Okonogi and Riangjanapatee [42] reported similar findings with solid lipid nanoparticles containing lycopene, a carotenoid akin to lutein, demonstrating that encapsulated lycopene was 100 times more stable than in solution. This result reflects a significant advancement in the stability of carotenoids, such as lutein, when they are encapsulated.

The stability study conducted at different temperatures assessed the behavior of these nanocapsules. Despite their sensitivity to higher temperatures, which affects droplet movement, these nanostructures show less tendency for droplet aggregation compared to larger-scale formulations like macroemulsions or lutein without adequate formulation [12,36,38]. The study concluded that there was no significant difference in the physicochemical aspects of samples stored at room temperature and in the refrigerator. PCL was considered promising as an encapsulating material, protecting lutein from environmental factors and maintaining nanoparticle stability for up to 30 days.

In the three assays studied, the LNCs exhibited antioxidant activities improved compared with WNC, with exception in the DPPH test that the results are statistically similar (between WNC and LNC-1). This difference can be explained because of steric effects of DPPH, increasing the difficulty in reacting with the radicals molecules. Therefore, the groups present in WNC also contribute distinctly to antioxidant activity of the particles. For the FRAP and DPPH assays, LNC-2 showed enhanced activity of lutein compared to free lutein, highlighting the relevance of nanotechnology in enhancing the antioxidant activity of lutein. In the ABTS•+ assay, a higher contribution to antioxidant activity was demonstrated for free lutein compared to LNC-1 and LNC-2 ($p<0.05$). However, notably, LNC-2 exhibited superior antioxidant activity across all three assays compared to LNC-1 and WNC. For all three assays conducted, the influence of lutein concentration in the nanocapsules was demonstrated. For instance, in the FRAP assay, LNC-2 (556.30 μg AA mL^{-1}) showed higher activity than LNC-1 (267.84 μg AA mL^{-1}). These results illustrate the ability of nanocapsules to protect bioactive compounds, such as lutein, while maintaining their antioxidant properties intact. The dependence on the loaded lutein concentration can be observed in the results exhibited.

Lutein, an oxygenated carotenoid, is one of the most essential xanthophylls part of the human diet. The importance of carotenoids is their antioxidant effects, mainly in $^1O_2$ quenching. The $ROO^{\bullet}$ are the only free radicals able to destroy the carotenoid completely, because the carotenoids, including lutein, have conjugated double bonds in their internal structure. The series of rotational and vibrational interactions with the solvent can result in the release of the newly acquired energy, returning the molecules to their ground state and enabling them to react and neutralize additional free radicals [43]. Lutein, and other carotenoids, have conjugated double bonds that can interact with electrophilic reagents, including reactive oxygen species (ROS) - both free radicals and non-radical species - contributing to decrease the oxidative stress. The mechanisms involved in these antioxidant reactions, usually, are electron transfer, donation of hydrogen and radical addition. However, it is most probable the predominance of the electron transfer mechanism [44]. It knowing about the mechanisms involved, it justifies the results shown, which in FRAP assay demonstrate clearly the contribution of antioxidant property of lutein in LNCs, because of predominance of electron transfer

in FRAP assay that evaluate reducing power of Fe^{3+} to Fe^{2+}. For other side, $DPPH^{\bullet}$ and $ABTS^{\bullet+}$ assays include mechanisms such as hydrogen atom transfer (HAT) and electron transfer (ET) - there is considerable discussion among researchers about this issue - and they are sterically hindered with the radicals center highly protected [45-47]. Thus, difficult the access of antioxidants present in nanocapsules.

A concentration-dependent decrease in cell viability was assessed in the 3T3 cell viability study, with a progressive reduction in the viability of cells as the concentration of LNC-1 and LNC-2 increased. These results suggest a correlation that varies with dose between lutein concentration and its impact on cell viability. Bolla and coauthors [48] conducted an investigation on the cytotoxicity of polymeric nanoparticles composed of PLGA-PEG-biotin, which contained lutein, in ARPE-19 cells. The analysis results revealed that both free and encapsulated lutein did not exhibit cytotoxic effects within the concentrations of 10, 20, and 50 µg/mL. Moreover, it was found that encapsulated lutein exhibited a lower rate of cytotoxicity compared to free lutein, suggesting that the nanoformulation was safe, effective, and non-toxic. This finding aligns with the results observed by Chittasupo and coauthors [49], where a similar phenomenon in ARPE-19 cells exposed to PLGA nanoparticles containing lutein in a cell viability assay. Even after a 72-hour analysis period, cell viability remained above 82% of the control when subjected to concentrations varying from 1 to 500 µg/mL of the sample in question. These findings indicated that the lutein nanoparticles exhibited excellent biocompatibility, showing no cytotoxicity *in vitro* at lower concentrations.

Our study significantly advances by not only focusing on the preparation and stability of lutein nanocapsules but also exploring their functionality and application in innovative ways. While Brum and coauthors [14] primarily examined basic physicochemical properties and stability under different storage conditions, we introduced advanced characterization techniques, such as FESEM, FTIR, and XRD, to better understand the nanocapsule structure and interactions. Additionally, our results highlighted the encapsulation's ability to enhance antioxidant activity and demonstrated its biocompatibility through cytotoxicity assays on fibroblasts. Most importantly, we paved the way for groundbreaking applications in anti-aging skincare, showing that encapsulated lutein not only maintains superior stability but also offers enhanced efficacy for topical delivery, marking a transformative step in the field of nanostructured antioxidant systems.

CONCLUSION

Lutein-loaded PCL nanocapsules were successfully produced, demonstrating advantageous physicochemical properties including a small nanometric size, low polydispersity index, and a negative zeta potential close to -30 mV. Additionally, the pH of the nanocapsules was found to be close to 5, making them suitable for skin application. FESEM images further confirmed the presence of a reservoir structure characteristic of nanocapsules, showcasing a smooth surface, rounded shape, and nanometric size. This was later confirmed by XRD and FTIR analyses.

Stability assessments indicated that storage in a refrigerator and room temperature is the most recommended method for preserving the physicochemical characteristics of lutein nanocapsules over time.

Nanoencapsulation enhances the antioxidant activity *in vitro* compared with free lutein and nanocapsules containing lutein show biocompatibility with fibroblasts at lower concentrations.

These findings suggest that PCL nanocapsules hold potential as effective nanocarriers for delivering lutein topically to skin, thus allowing for the delivery of its therapeutic benefits. Additionally, this research offers important information for the creation of dermocosmetic products that incorporate nanotechnology.

Funding: Authors are grateful to CAPES (88887.694782/2022-00) for financial support.
Acknowledgements: State University of Ponta Grossa (UEPG); C-Labmu (UEPG); Grateful to CAPES for supplying the tools, facilities, and other resources essential for this study, as well as for fostering research and scientific advancement in Brazil.
Conflicts of Interest: The authors declare no conflict of interest.

REFERENCES

1. Dai X, Hu Y, Jiang L, Lei L, Fu C, Wu S, et al. Decreased oxidative stress response and oxidant detoxification of skin during aging. Mech Ageing Dev. 2023 Dec;216:111878.
2. Quan T. Molecular insights of human skin epidermal and dermal aging. J Dermatol Sci. 2023 Nov;112(2):48-53.
3. Junqueira LCU, Carneiro J. Basic Histology. Guanabara Koogan [Internet]. 2013;12:65-96. Available from: https://www.yumpu.com/pt/document/read/58279120/histologia-basica-texto-e-atlas-12-edicao-junqueira-amp-carneiro.
4. Vênus M, Waterman J, Mcnab I. Basic physiology of the skin. Surgery (Oxford) 2011 29(10):471-4.

5. Sharma A, Kuhad A, Bhandari R. Novel nanotechnological approaches for treatment of skin-aging. J Tissue Viability. 2022 Aug;31(3):374-86.
6. Mohd Zaid NA, Sekar M, Bonam SR, Gan SH, Lum PT, Begum MY, et al. Promising Natural Products in New Drug Design, Development, and Therapy for Skin Disorders: An Overview of Scientific Evidence and Understanding Their Mechanism of Action. Drug Des Devel Ther. 2022 Jan;16:23-66.
7. Flieger, J, Raszewska-Famielec M, Radzikowska-Büchner E, Fliege W. Skin Protection by Carotenoid Pigments. Int. J Mol Sci 2024;*25*:1431.
8. De Ávila L, Primo FT. The use of oral antioxidants in photoprotection: a systematic review. Vittalle – J Health Sci. 2021;33(2):97-108.
9. Kotake-Nara E, Nagao A. Absorption and metabolism of xanthophylls. Mar Drugs. 2011;9(6):1024-37.
10. Mitra S, Rauf A, Tareq AM, Jahan S, Emran TB, Shahriar TG, et al. Potential health benefits of carotenoid lutein: An updated review. Food Chem Toxicol. 2021 Aug;154:112328.
11. Nikhat A, Hasan N, Iqbal Z, Kesharwani P, Talegaonkar S. Enhanced transdermal delivery of lutein via nanoethosomal gel: Formulation optimization, in-vitro evaluation, and in-vivo assessment. J Drug Deliv Sci and Technol. 2022;73:103447.
12. Schaffazick SR, Guterres SS, Freitas L de L, Pohlmann AR. Characterization and physicochemical stability of nanoparticulate polymeric systems for drug delivery. Quim Nova [Internet]. 2003 Sep;26(5):726–37. Available from: https://doi.org/10.1590/S0100-40422003000500017.
13. Maleki A, Karimpour A, Maleki Dizaj S. The role of mechanical engineering in the development of nano drug delivery systems; a review. Int J Nanodimens. 2018;9(1):1-6.
14. Brum A, Dos Santos P, Silva M, Paese K, Guterres S, Costa T, et al. Lutein-loaded lipid-core nanocapsules: Physicochemical characterization and stability evaluation. Colloids Surf A Physicochem Eng Asp. 2017 mar;522.
15. Balić A, Mokos M. Do We Utilize Our Knowledge of the Skin Protective Effects of Carotenoids Enough? Antioxidants (Basel). 2019 Jul 31;8(8):259.
16. Roberts RL, Green J, Lewis B. Lutein and zeaxanthin in eye and skin health. Clin Dermatol. 2009 Mar-Apr;27(2):195-201.
17. Deng S, Gigliobianco MR, Censi R, Di Martino P. Polymeric Nanocapsules as Nanotechnological Alternative for Drug Delivery System: Current Status, Challenges and Opportunities. Nanomaterials (Basel). 2020 Apr 28;10(5):847.
18. Fessi H, Puisieux F, Devissaguet JPH, Ammoury N, Benita S. Nanocapsule formation by interfacial polymer deposition following solvent displacement. Inter J. of Pharm X. 1989;55:R1-4.
19. Berker KI, Güçlü K, Tor I, Apak R. Comparative evaluation of Fe(III) reducing power-based antioxidant capacity assays in the presence of phenanthroline, batho-phenanthroline, tripyridyltriazine (FRAP), and ferricyanide reagents. Talanta. 2007 May 15;72(3):1157-65.
20. Brand-Williams W, Cuvelier ME, Berset C. Use of a free radical method to evaluate antioxidant activity. Food Sci and Tech. 1995;28:25-30.
21. Re R, Pellegrini N, Proteggente A, Pannala A, Yang M, Rice-Evans C. Antioxidant activity applying an improved ABTS radical cation decolorization assay. Free Radic Biol Med. 1999 May;26(9-10):1231-7.
22. Shu X, Zhang L, Liao W, Liu J, Mao L, Yuan F, et al. Nanostructured lipid carriers (NLCs) stabilized by natural or synthetic emulsifiers for lutein delivery: Improved physicochemical stability, antioxidant activity, and bioaccessibility. Food Chem. 2023 Mar 1;403:134465.
23. Vásquez Marcano RGDJ, Tominaga TT, Khalil NM, Pedroso LS, Mainardes RM. Chitosan functionalized poly (ε-caprolactone) nanoparticles for amphotericin B delivery. Carbohydr Polym. 2018 Dec 15;202:345-54.
24. Camargo G, Ferreira L, Schebelski D, Lyra A, Barboza F, Carletto B, et al. Characterization and In Vitro and In Vivo Evaluation of Tacrolimus-Loaded Poly(ε-Caprolactone) Nanocapsules for the Management of Atopic Dermatitis. Pharmaceutics. 2021 Nov;13:2013.
25. Do Prado Silva JT, Geiss JMT, Oliveira SM, Brum EDS, Sagae SC, Becker D, et al. Nanoencapsulation of lutein and its effect on mice's declarative memory. Mater Sci Eng C Mater Biol Appl. 2017 Jul 1;76:1005-11.
26. Jarai B, Kolewe E, Stillman Z, Raman N, Fromen C. Polymeric Nanoparticles. Nanopaticles Biomed Applic. 2020 Jan; 308-24.
27. Danaei M, Dehghankhold M, Ataei S, Hasanzadeh Davarani F, Javanmard R, Dokhani A, et al. Impact of Particle Size and Polydispersity Index on the Clinical Applications of Lipidic Nanocarrier Systems. Pharmaceutics. 2018 May 18;10(2):57.
28. Bhatia S. Nanoparticles Types, Classification, Characterization, Fabrication Methods and Drug Delivery Applications. 2016 sep; 1:33-93.
29. Li J, Wang X, Yu D, Zhoujin Y, Wang K. Molecular complexes of drug combinations: A review of cocrystals, salts, coamorphous systems and amorphous solid dispersions. Int J Pharm. 2023 Dec 15;648:123555.
30. Zanetti M, Mazon LR, de Meneses AC, Silva LL, de Araújo PHH, Fiori MA, et al. Encapsulation of geranyl cinnamate in polycaprolactone nanoparticles. Mater Sci Eng C Mater Biol Appl. 2019 Apr;97:198-207.
31. Schmid-Wendtner MH, Korting HC. The pH of the skin surface and its impact on the barrier function. Skin Pharmacol Physiol. 2006;19(6):296-302.

32. Carneiro-da-Cunha M, Cerqueira M, Souza B, Teixeira J, Vicente A. Influence of concentration, ionic strength and pH on zeta potential and mean hydrodynamic diameter of edible polysaccharide solutions envisaged for multinanolayered films production. Carbohydr. Polym. 2011 Jun;85:522-8.
33. Carter P, Narasimhan B, Wang Q. Biocompatible nanoparticles and vesicular systems in transdermal drug delivery for various skin diseases. Int J Pharm. 2019 Jan 30;555:49-62.
34. Ferreira LM, Cervi VF, Sari MHM, Barbieri AV, Ramos AP, Copetti PM. Diphenyl diselenide loaded poly(ε-caprolactone) nanocapsules with selective antimelanoma activity: Development and cytotoxic evaluation. Mater Sci Eng C Mater Biol Appl. 2018 Oct 1;91:1-9.
35. Yingngam B, Navabhatra A, Pharikarn P, Vonganakasame K, Kanoknitthiran V, Rungseevijitprapa W, et al. Optimization of menthol-loaded nanocapsules for skin application using the response surface methodology. J. Drug Deliv Sci Tech. 2019 Jul;53:101138.
36. Campos PM, Praça FG, Mussi SV, Figueiredo SA, Fantini MCA, Fonseca MJV, et al. Liquid crystalline nanodispersion functionalized with cell-penetrating peptides improves skin penetration and anti-inflammatory effect of lipoic acid after in vivo skin exposure to UVB radiation. Drug Deliv Transl Res. 2020 Dec;10(6):1810-28.
37. Jiao Y, Shi L, Li D, Chang Y. Lutein-loaded glycosylated zein nanoparticles-Preparation, characterization, and stability in functional drink. Food Sci Tech. 2023 Nov 1;187:115308.
38. Lopes BA, Boscardin PD, Campos PM. Development and Characterization of Nanoemulsion Containing Volatile Oil of Matricaria recutita L. Braz arch biol technol [Internet]. 2023;66(spe):e23230576. Available from: https://doi.org/10.1590/1678-4324-ssbfar-2023230576.
39. Diyanat M, Saeidian H, Baziar S, Mirjafary Z. Preparation and characterization of polycaprolactone nanocapsules containing pretilachlor as a herbicide nanocarrier. Environ Sci Pollut Res Int. 2019 Jul;26(21):21579-88.
40. De Melo N, Grillo R, Rosa A, Fraceto L, Filho N, de Paula E, et al. Development and characterization of poly (L-lactide) nanocapsules containing benzocaine. Quim. Nova 33:65-9.
41. Álvarez-Henao MV, Saavedra N, Medina S, Jiménez Cartagena C, Alzate LM, Londoño-Londoño J. Microencapsulation of lutein by spray-drying: Characterization and stability analyses to promote its use as a functional ingredient. Food Chem. 2018 Aug 1;256:181-87.
42. Okonogi S, Riangjanapatee P. Physicochemical characterization of lycopene-loaded nanostructured lipid carrier formulations for topical administration. Int J Pharm. 2015 Jan 30;478(2):726-35.
43. Gulcin İ. Antioxidants and antioxidant methods: an updated overview. Arch Toxicol. 2020 Mar;94(3):651-715.
44. Pisoschi AM, Pop A. The role of antioxidants in the chemistry of oxidative stress: A review. Eur J Med Chem. 2015 Jun 5;97:55-74.
45. Schaich K, Tian X, Xie J. Hurdles and Pitfalls in Measuring Antioxidant Efficacy: A Critical Evaluation of ABTS, DPPH, and ORAC Assays. J. Funct Foods. 2015;14:111–25.
46. Shahidi F, Zhong Y. Measurement of Antioxidant Activity. J. Funct. Foods. 2015;18:757–81.
47. Lichtenberg D, Pinchuk I. Oxidative stress, the term and the concept. Biochem Biophys Res Commun. 2015 Jun 5;461(3):441-4.
48. Bolla PK, Gote V, Singh M, Patel M, Clark BA, Renukuntla J. Lutein-Loaded, Biotin-Decorated Polymeric Nanoparticles Enhance Lutein Uptake in Retinal Cells. Pharmaceutics. 2020 Aug 24;12(9):798.
49. Chittasupho C, Posritong P, Ariyawong P. Stability, Cytotoxicity, and Retinal Pigment Epithelial Cell Binding of Hyaluronic Acid-Coated PLGA Nanoparticles Encapsulating Lutein. AAPS PharmSciTech. 2018 Dec 17;20(1):4.